Wojciech Łużny,
Maciej Śniechowski

Faculty of Physics and Nuclear Techniques,
University of Mining and Metallurgy,
al. Mickiewicza 30, 30-059 Cracow, Poland
Sniechowski@novell.ftj.agh.edu.pl

The role of water content for the emeraldine base structure

Abstract

A series of the polyaniline samples in the emeraldine base form was synthesised in various conditions, and was then subjected to the experimental X-ray diffraction measurements and a computer modelling study. Additionally, the elemental analysis technique was also used. Reasonable models of the crystalline structure of various types of the polymer systems (known as EB-1 and EB-2) are proposed. The presence of water molecules in the crystalline regions of polyaniline is discussed, and the significant role of these molecules for the structural properties of emeraldine base samples is explained.

Key words: *X-ray diffraction, crystalline structure, polyaniline, water absorption*

1. Introduction

A molecule of the emeraldine base (EB) form of polyaniline (PANI) consists of alternating reduced and oxidised segments, and may be described by the general formula shown in Figure 1. PANI is one of the most intensively studied conjugated polymers. Nevertheless, the number of papers dealing with the structural properties of an EB, which is the starting point for all further treatments and modifications, is still rather low, particularly regarding X-ray diffraction studies.

Detailed studies of water absorption process in both types of PANI suggest that a certain amount of water molecules may exist in even dried samples. The content of water, as determined by the use of several experimental techniques (for example TGA, DSC, NMR and elemental analysis), varies from 5 to 15% [7-10]. Several hypotheses concerning the mechanism of water presence in PANI samples have been proposed. In ES form, the water molecules are absorbed onto the amine sites of polyaniline. In EB form, the water molecules are bonded with amine or imine nitrogen atoms into a polymer backbone. There are two types of absorbed water molecules, mobile (reversible) and fixed (irreversible) [9]. The mobile molecules are attached by one hydrogen bond, and the fixed molecules create two hydrogen bonds. Water molecules may be bound either to the polymer backbone or to the fixed water molecule. In dried samples fixed water molecules are still present. The mobile water molecules may be removed from PANI by heating up to 70-150 ^{0}C, whereas fixed water molecules escape from PANI only simultaneously with polymer decomposition. The other hypothesis states that there are two types of mobile (reversible) absorbed water [8]. The molecules of the first type can be removed from PANI by a flow of nitrogen at room temperature, and have the activation energy of desorption of about 5 kcal/mol. These water molecules interact with the polymer by hydrogen bonding between a hydrogen atom of amine centre in EB and an oxygen atom of water. The second form of water molecules exhibits a greater energy of desorption, of about 15-18 kcal/mol. The water molecules are attached by a hydrogen bond between its hydrogen atom and the nitrogen atom of EB, and these may escape at the temperature of 70-150 ^{0}C.

2. Sample preparation

Emeraldine salt was chemically synthesised by oxidation of aniline (not distilled or vacuum distilled) with ammonium peroxidisulphate ($(NH_4)_2S_2O_8$), according to the standard method [11]. This process was carried out under controlled conditions by adding a persulphate solution (46 g $(NH_4)_2S_2O_8$ in 1M HCL) to the stirred aniline solution (88 ml of aniline in 1M HCL). The reaction mixture was stirred and maintained at a constant temperature (*i.e.* 0C^o or 20C^o) for 1.5 hours. The mixture was then filtered with a Büchner funnel and washed with distilled water and methanol until the filtrates were colourless. In order to obtain the emeraldine base samples, the as-synthesised ES powder was immersed in 2000 ml of 0.1 M NH_4OH and stirred for 15 hours. The EB powder (obtained as described above) was washed using a Soxhlet apparatus or a Büchner funnel. The following solvents were applied: methanol, chloroform and THF.

3. Experimental

The powder samples were measured with two X-ray wide-angle diffractometers at room temperature. Both the diffractometers, the HZG-4 and the SEIFERT-FPM XRD 7, were equipped with a copper X-ray tube (wavelength -0.154 nm) and a nickel filter. Diffracted intensity was collected for 2Θ angles from 2^o to 50^o with the step of 0.05^o.

Figure 2 shows the diffraction patterns obtained for selected samples of emeraldine base. All x-ray powder profiles correspond to those reported previously, and they exhibit two components, due to scattering by amorphous and crystalline phases.

The diffraction patterns of PANI EB may generally be divided into two groups by the different positions of the main Bragg reflections. For the first type (named EB-1), the crystalline component of the diffraction profile shows characteristic Bragg reflections near 15, 20 and 24^0 (2Θ). The diffraction pattern typical of the second type of PANI EB is characterised by the predominant

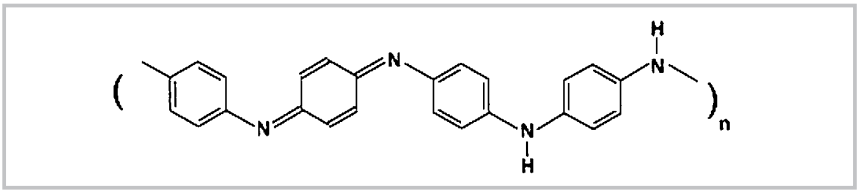

Figure 1. *Schematic illustration of polymer repeating unit for emeraldine base.*

high maximum near 19^0 (2Θ); the other reflections near 15 and 23^0 are less intense. This type of PANI EB was named EB-2.

As-synthesised PANI always exhibits the EB-1 form. However, the diffraction patterns collected for several samples may differ remarkably: the ratio of a crystalline component to an amorphous one changes due to the different degree of crystallinity.

The EB-1 samples extracted by THF or NMP exhibit the diffraction profiles typical of the EB-2 form of PANI, which suggests that these types of solvents may induce a structural transition from the EB-1 to EB-2 form of PANI. However, if the extraction process is performed with solvents such as methanol or chloroform, no such structural transition takes place. The only effect of this process is the enhancement of the degree of crystallinity, which is proved in the X-ray diffraction results by the significant increase in the intensity of the crystalline component.

The diffraction patterns typical of the EB-2 form, recorded for several samples, are almost identical. The predominant peak at 22.19^0 has the same intensity for all samples; the only difference is related to the reflection at 22.12^0. For the soluble fraction (in THF, for example) this maximum vanishes, whereas for the insoluble fraction this peak is well visible as a relatively broad maximum (see Figure 2).

Coming back to the EB-1 form of PANI, one can observe that the diffraction patterns typical of this form may be divided into two groups, regarding their shape in the region of lower diffraction angles. This effect has been not explained in the literature so far. For the first kind of EB-1 type (which has been named EB-1α), the diffraction patterns exhibit two distinct peaks in this region, namely at 6 and 9^0 (2Θ). The second kind of EB-1 type, described here as EB-1β, is also characterised by two peaks, but located at 9 and 12^0 (2Θ). Sometimes, the broad maximum at 12^0 may not be well separated from the next broad maximum at 15^0. It should be underlined that for the as-synthesised PANI EB samples, it is possible to obtain the diffraction patterns of both EB-1α and EB-1β types.

For further discussions and diffraction data processing, we performed the typical procedure of separating the crystalline component. The amorphous component of all diffraction patterns has been approximated by the Lorentzian

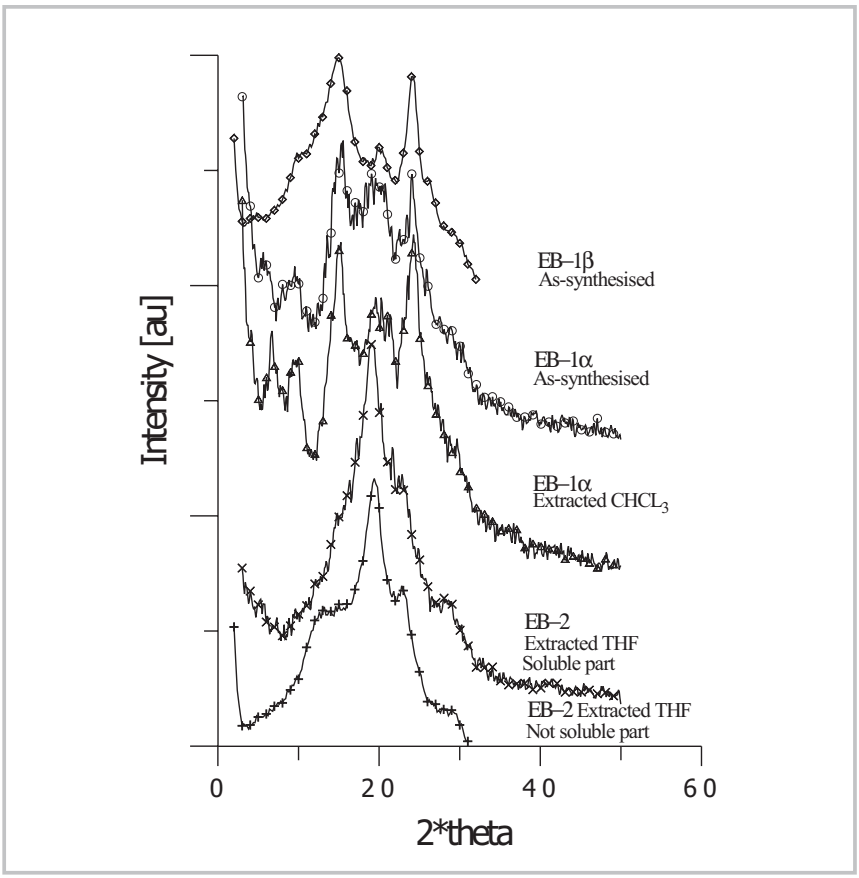

Figure 2. *Diffraction patterns for selected samples.*

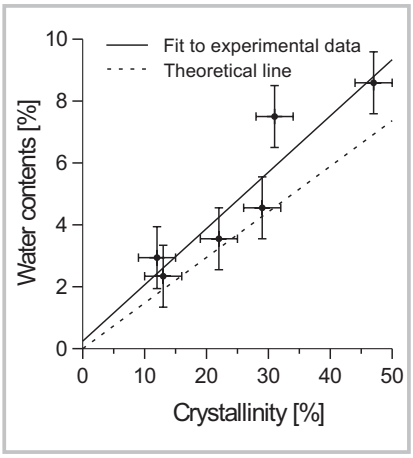

Figure 3. *Correlation between the degree of crystallinity and samples of emeraldine base. The mass deficiency for PANI EB.*

(identical for all EB samples), whereas the crystalline components have been represented as the sum of the Gaussians. Thanks to this procedure, we were able to estimate the degree of crystallinity of all samples investigated.

The EB samples measured by use of the X-ray diffraction technique have been subjected to elemental analysis in order to determine the concentrations of all the basic elements, C, H, and N. The sum of resulting concentrations of all elements is always less than 100. As discussed above, a distinct amount of water can be present in the PANI samples. Regarding their mass, the water molecules consist mainly of oxygen atoms, whose share cannot be determined by elemental analysis directly, but can be estimated from the percentage deficiency of mass only. The water contents estimated on the base of elemental analysis were confirmed by thermal analysis. We have assumed tentatively that for one repeating unit of PANI EB (composed of four aromatic rings), there are four molecules of water.

The next stage of our discussion is based on the observation that the samples with higher crystallinity show the higher value of mass deficiency. Therefore, it is reasonable to assume that the water molecules are located mainly in the crystalline areas of the PANI system. If one now calculates the theoretical shares of the basic elements for several degrees of crystallinity (assuming that there are no water molecules in the amorphous phase of PANI), it is possible to observe a striking agreement between the results of such calculations and the experimental results, particularly those obtained for EB-2 samples. Of course, total neglect of the water contents in the

amorphous regions cannot be practically achieved, and therefore the experimental mass deficiency is (more or less) higher than the value obtained from theoretical calculations. The important correlation between the degree of crystallinity and the mass deficiencyindicated above is shown in Figure 3 together with the results of these theoretical speculations.

All these results enabled us to conclude that the water molecules are an inherent component of the PANI EB crystalline structure, and that their presence should be taken into account in further structural investigations.

4. Computer modelling

The repeating unit of PANI EB consists of three benzenoid rings (*B*) and one quinoid ring (*Q*). This leads to an asymmetric unit of the type *BBQB*. As we have already noted, it is reasonable to assume that there are four molecules of water per one such unit. These molecules are located between the PANI chains; they bond by hydrogen bonds both to the nitrogen atoms of PANI and to themselves.

We have taken into account two possibilities concerning the conformation of the polymer chains. In the first case, the quinoid rings are co-planar with the plane defined by the nitrogen atoms, and the benzenoid rings are tilted alternately by an angle of 0 to 30^0. For the second case, all rings are tilted alternately. Both models of conformation lead to almost identical results.

We have worked with a low-symmetric, triclinic unit cell. The parameters of the cell were selected for each case in such a way that the positions of the crystalline reflections were correct.

4.1. Models of the EB-1 crystalline structures

In this case, it was necessary to choose such parameters of the unit cell that the interplanar distances related to the crystalline reflections for 6 and 9^0 appear in the structure. We obtained the following set of these parameters: a = 1.25, b = 0.583, c = 1.923 nm, and α = 90, β = 45, $\gamma = 93^0$.

The unit cell consists of two PANI chains, parallel to the *z* direction. Therefore, the dimensions of the aromatic rings and other parameters of covalent bonds have determined the lattice constant *c*. The identical angle N = 40^0 tilts both chains about their axes. The relative intensity of the main crystalline peaks (for 22.15, 20 and 24^0) are very sensitive to the assumed N angle, which enabled us to determine its value. Of course, the unit cell containing no water molecules could be reduced twice in the *x* direction. Such a structural model allows description of the relative intensity and the crystalline indices of three reflections mentioned above: (0 1 0), (2 0 0) and (2 –1 0), respectively.

Straight PANI chains, with no side groups, do not form crystal planes separated by large distances which could be responsible for lower angle diffraction peaks. Water molecules periodically ordered along the polymer chains may create such planes. These molecules are located in the neighbourhood of the nitrogen atoms. For the correct parameters of the unit cell, it is possible to obtain new diffraction reflections, e.g. (1 0 2), and as alternatives (0 0 1) or (0 0 2). Their positions in 2Θ are equal to 9, 6 and 12^0, respectively, and their relative intensity is very sensitive to the arrangement of water molecules within the unit cell. Of course, the ratio of the integral intensity of all these peaks originating from the existence of the water molecules to the integral intensity of the peaks originating from the polymer chains depends on the water contents. For the present models, there is one water molecule for one nitrogen atom, and therefore the mass share of water in the crystalline phase of the whole system is about 12%. Such an assumption is reasonable from the physical point of view, because it is in agreement with the elemental analysis results, which have shown that the total content of water (both in a crystalline and in an amorphous phase) can be estimated as *ca.* 6%. Naturally the degree of crystallinity is relatively low, but we have assumed that the majority of water is located in the crystalline regions.

As mentioned above, there are two types of EB-1 diffraction patterns, named EB-1α (with crystalline peaks for 6 and 9^0) and EB-1β (with crystalline peaks for 9 and 12^0). The results of the computer modelling allow us to state that these two structures can be distinguished by the arrangement of the water molecules in the structure. If these molecules are grouped for every fourth nitrogen atom, we obtain the reflection (0 0 1) for 2Θ equal to -6^0. Alternatively, the reflection (0 0 2) for 2Θ equal to -12^0 is observed, if the water molecules are bonded to every second nitrogen atom. Of course, the reflections (0 0 1) and (0 0 2) cannot be observed simultaneously due to the reflection conditions. Both models of the PANI EB-1 structure are shown in Figures 5 and 6.

The calculated density for both models is about 1.37 g/cm^3. The comparison of the calculated diffraction patterns with their experimental 'partners' is presented in Figures 6a and 6b.

4.2. Model of the EB-2 crystalline structure

We started from the same triclinic unit cell as for the EB-1 structure, but due to the different positions of the crystalline reflections we had to slightly alter the cell parameters. The set of parameters which we obtained for the EB-2 structure is as

Table 1. *Structure parameters for PANI EB models.*

PANI	Lattice constant [nm] a b c			Cell angles [degree] α β γ			angle φ
EB-1	1.25	0.583	1.923	90	45	93	40
EB-2	1.25	0.583	1.923	90	48	98	30

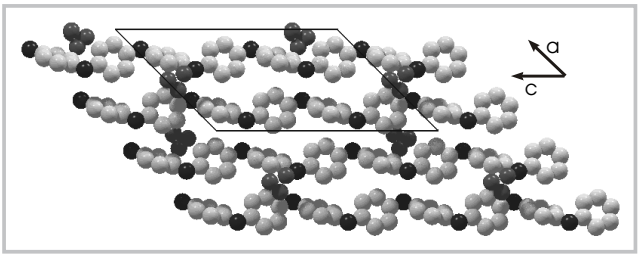

Figure 4. *Model of PANI EB-1α structure shown in b direction.*

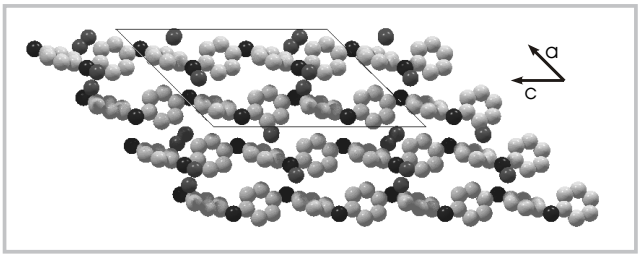

Figure 5. *Model of PANI EB-1β structure shown in b direction.*

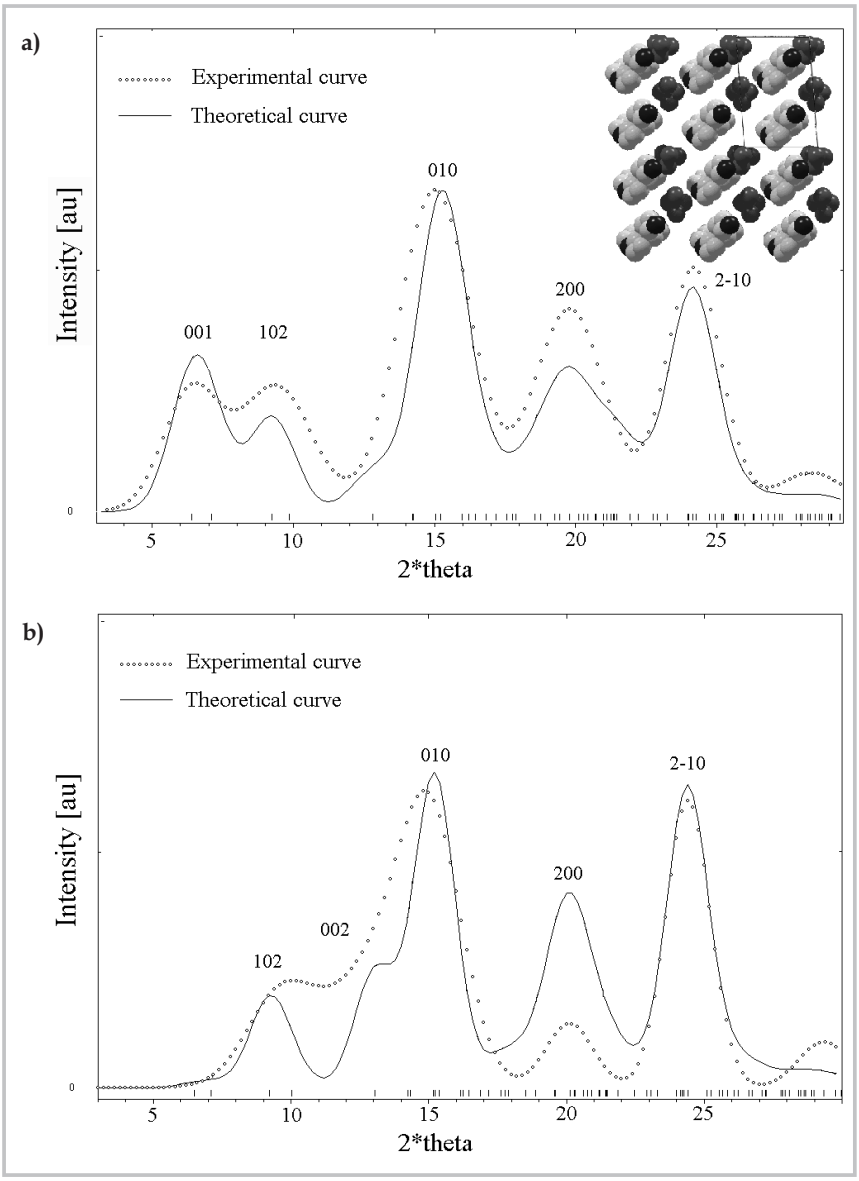

Figure 6. *Comparison of the calculated diffraction pattern with the crystalline component of experimental curve for a) PANI EB-1α (inset: model structure shown in c direction). b) PANI EB-1β.*

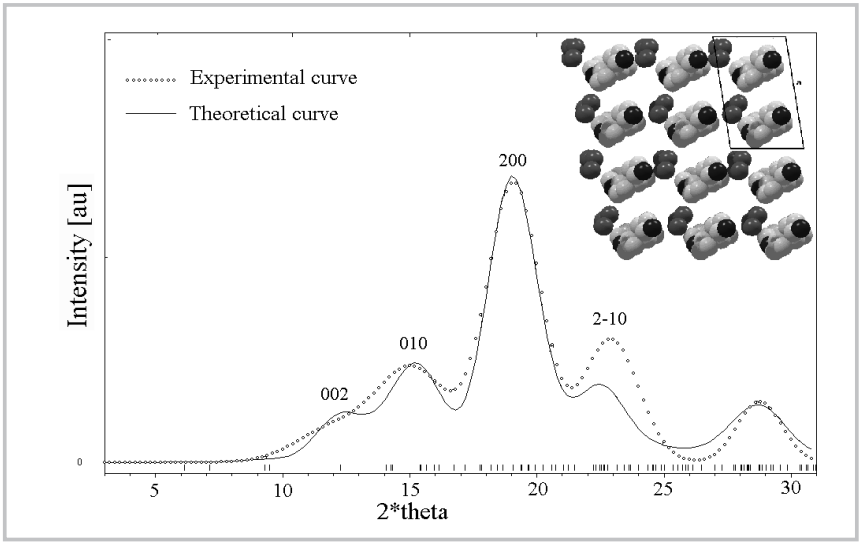

Figure 7. *Comparison of the calculated diffraction pattern with the crystalline component of experimental curve for PANI EB-2 (inset: model structure shown in c direction).*

follows: $a = 1.25$, $b = 0.583$, $c = 1.923$ nm, and $\alpha = 90$, $\beta = 48$, $\gamma = 98^0$. Because the relative intensity of the three main reflections for 2Θ equal to -15, 19 and 23^0 (typical of the EB-2 structure) is very different than the relative intensity of the three main peaks visible for EB-1, it was necessary also to change the relative arrangement of the PANI chains within the unit cell. Reasonable agreement is achieved if all chains are tilted by an angle N of $.30^0$. For such a model structure, it is possible to describe both the positions as well as the relative intensity of these three main peaks with the crystal indices (0 1 0), (2 0 0) and (2 –1 0) respectively. As in the case of EB-1 structure, the origin of the broad reflection for 2Θ equal to -12^0 is explained by the presence of the water molecules in the structure which are bonded to every second nitrogen atom. Therefore, this reflection has the crystal indices (0 0 2) again, and in this case there is no reflection (0 0 1) for 2Θ equal to -6^0. The calculated density of the EB-2 model structure (shown in Figure 7 in insert) is about 1.33 g / cm^3. The comparison of the calculated diffraction pattern with the crystalline component of the experimental one is presented in Figure 7.

5. Conclusions and discussion

The differences observed in the relative intensities of the calculated and experimental diffractograms should be put together with the well-known, significant differences in the relative intensities of experimental diffraction patterns recorded for various samples. Thus, it is hard to expect the agreement between calculated and experimental diffraction traces to be excellent. However, it should be realised that the models presented in this work are only hypothetical (they are not unique), and other models, for which this agreement would be better, could replace them.
-By the comparison of two models obtained for EB-1 and EB-2 it is possible to state that a very delicate change of the unit cell parameters implies remarkably big changes in the shape of a diffraction pattern. Therefore we have been able to describe two (or even three) different structures within one simple model, with only very slight modifications. Such a result should not come as a great surprise because the change from EB-1 to EB-2 structure is forced by the extraction from the selected solvents, which cannot change the molecular structure of the polymer backbone, though they cannot induce any significant change in the crystalline structure of the system. The lattice

constants of both models are identical, and the differences in the positions of the crystalline reflections are related to very small changes in the cell angles. The tilt angle N of the chains (about their axis) is an important parameter of our models; the small change of its value allows quite significant differences between the relative intensity of the crystalline peaks to be described. For the EB-1 type of the diffraction pattern, two reflections (0 1 0) and (2 –1 0) predominate, and the reflection (2 0 0) is much lower. The change of the angle N by only 10 degrees (from 40 to 30^0) implies the inversion of the situation, and for the case of EB-2 type one reflection (2 0 0) predominates, whereas the two remaining peaks exhibit lower intensity.

Introducing the water molecules to the crystalline structure of PANI EB allowed us to explain the origin of the lower angles diffraction peaks as the reflections (0 0 1), (1 0 2) and (0 0 2). In the experimental diffraction patterns, these peaks are usually broader than the calculated ones, and this effect is easy to explain by the fact that in the real system the ordering of the water molecules along the PANI chains is not so perfect as in the theoretical model. The correlation length of an ordered area of the water molecules has been estimated from the broadening of the diffraction reflection (by use of Scherrer's formula) as *ca* 9 nm.

The creation of two different types of EB-1 structures, namely EB-1α and EB-1β, is related to the fact that there are two ways of absorption ('entrapping') of water molecules in the structure of PANI EB (as described in the introduction). The existence of the water molecules with different values of activation energy of desorption allows gradual removal of the water molecules from the system. This effect is very well confirmed by the fact that for the EB samples dried at elevated temperatures or during longer times, the diffraction patterns change and the lower angle diffraction peaks vanish.

The main benefit of our work is that we have been able to describe different structures, which exhibit quite different diffraction patterns, within one very simple model, containing only two PANI chains in its asymmetric unit. Secondly, we have demonstrated a new and very interesting relationship between the degree of crystallinity of PANI EB samples and the mass deficiency occurring in the elemental analysis results (see Figure 3). This effect has been explained by the entrapping of the water molecules mainly in the crystalline regions of the polymer; this hypothesis is supported both by the theoretical calculations as well as by our computer modelling results.

Our conclusions are in very good agreement with the very recent results of the theoretical calculations and photoluminescence studies presented by J.Y. Shimano and A.G. MacDiarmid [12].

We can state that the results of our X-ray diffraction measurements, computer modelling and elemental analysis investigations constitute a coherent and logical unity, and provide a reasonable explanation for the PANI EB crystal structure.

Acknowledgements

We acknowledge KBN Grant No. 2P03B04116 of the Polish State Committee for Scientific Research for W. Łużny and WIMiC AGH Grant No. 11.11.160.203 of thge University of Mining and Metallurgy (for J.L.), which financially supported this work. We are indebted to Dr W. Kraus and Dr G. Nolze (Berlin) for making the computer program POWDERCELL available. The fruitful discussions with Professor A.G. MacDiarmid are greatly acknowledged.

❑

References

1. *Pouget J.P., Józefowicz M. E., Epstein A.J., Tang X., MacDiarmid A.G.; Macromolecules 24 (1991) 779*
2. *Laridjani M., Epstein A.J.; Eur.Phys.J. B 7 (1999) 585*
3. *Laridjani M., Pouget J.P., Scherr E.M., MacDiarmid A.G., Józefowicz M. E., Epstein A.J.; Macromolecules 25 (1992) 4106*
4. *Józefowicz M. E., Epstein A.J., Pouget J.P., Masters J.G., Ray A., Sun Y., Tang X., MacDiarmid A.G.; Synthetic Metals, 41-43 (1991) 723-726*
5. *Winokur M.J., Mattes B.R.; J. of Reinforced Plastics and Composites, 18 (1999) 875*
6. *Winokur M.J., Mattes B.R.; Macromolecules 31 (1998) 8183*
7. *Alix A., Lemoin V., Nechtschein M., Travers J.P., Menardo C.; Synthetic Metals, 29 (1989) E457-E462*
8. *Matveeva E.S., Diaz Calleja R., Parkhutik V.P.; Synthetic Metals 72 (1995) 105-110*
9. *Lubentsov B.Z., Timofeeva O.N., Khidekel M.L.; Synthetic Metals 45 (1991) 235-240*
10. *Lubentsov B.Z., Timofeeva O.N., Saratovskikh S., Krinichnyj V.; Synthetic Metals 47 (1992) 187-192*
11. *Chiang J.C., MacDiarmid A.G.; Synthetic Metals 13 (1986) 193*
12. *Shimano J.Y., MacDiarmid A.G.; Proceedings of ICSM'2000, Gastein, Austria, to be published in Synthetic Metals*

❑ ***Received 14.01.2003, Revieved 05.05.2003***